Macroporous smart gel based on pH-sensitive polyacrylic polymer for the development of large size artificial muscle with linear contraction

Vincent Mansard

Journal Name

ARTICLE TYPE

Cite this: DOI: 00.0000/xxxxxxxxxx

Macroporous smart gel based on pH-sensitive polyacrylic polymer for the development of large size artificial muscle with linear contraction†

Vincent Mansard*[a]

Received Date
Accepted Date

DOI: 00.0000/xxxxxxxxxx

The physics of soft matter can contribute to the revolution in robotics and medical prostheses. These two fields requires the development of artificial muscles with behavior close to the biological muscle. Today, the artificial muscles rely mostly on active materials, which can deform reversibly. Nevertheless transport kinetic is the major limit for all of these materials. These actuators are only made of thin layer of active material and using large thickness dramatically reduces the actuation time. In this article, we demonstrate that porous material reduces the limit of transport and enables to use large volume of active material. We synthesis a new active material: a macroporous gel, which is based on polyacrylic acid. This gel show very large swelling when we increase the pH and the macroporosity dramatically reduces the swelling time of centimetric samples from one day to 100 s. We characterize the mechanical properties and the swelling kinetics of this new materials. This material is well adapted for soft robotic because of its large swelling ratio (300 %) and its capacity to apply a pressure of 150 mbar when swelling. We demonstrate finally that this material can be used into a McKibben muscle producing linear contraction, which is particularly adapted for robotics. The muscle contracts by 9 % of its initial length within 100 s—which corresponds to the gel swelling time.

Robotic is one of the major upcoming industrial revolution. Heavy industry already relies on robotic. Humanoid robots will closely help human. Exoskeleton and prosthetic device will give back a mobility to disabled people. The internet of thing will bring new tools, which can physically interact with their environment. The robotic revolution is possible thanks to the development of computer science and artificial intelligence but robots are not a challenge only for computer scientist. Robots are—first of all—a complex and precise mechanical system.

Unfortunately, up to now, these systems fail to meet their promises. They are heavy, with a poor energy efficiency and often too stiff to be safe for close interaction. For example the most advanced artificial heart weight 900 g—3 times a human heart—plus 3 kg of battery[1].

Surprisingly, the limit does not come from the computer but from the machinery[2]. Actuators used in robotic are highly unadapted. Robotic systems are biomimetic but rely on electrical or hydraulic motors very different from biological muscles. Their integration requires state of the art mechanics and, despite this, robots are not efficient enough for having an impact beyond industry. There is a vital need for a technological leap in actuation.

The research on innovative actuators—also called artificial muscles—is very active and several strategies can be identified. Soft pneumatic muscles[3–6] are probably the simplest systems. The actuation is due the inflation of an air chamber. The specific design of the chamber enables bending, twisting or linear contraction. This strategy is gaining momentum as it is cheap and quick. Nevertheless, these muscles require heavy air compressor, and controlling the pressure is complex and with a poor energy efficiency.

The other artificial muscles rely on mechanically active materials, where it is possible to trigger a reversible deformation. Different type of active material have been used. Shape memory alloys[7,8] and liquid crystal elastomers[9,10] expand or bend because of a temperature-induced phase transition. Conductive polymers[11] reversibly swell—by up to 30 %—because of electrically-controlled redox reaction inducing migration of ion in or out of the polymer. Dielectric elastomers is a compliant capacitor made of a thin sheet of elastomer sandwiched between two electrodes. It get deform under high voltage (1-10 kV).

Smart polymer gels are another class of active materials[12–18], which can reversibly swell by absorbing solvent when the chemical environment—pH, salinity, type of solvent or temperature—is modified. They are particularly interesting because they show very large swelling amplitude. This swelling is due to a modification of the affinity of the polymer for the solvent. The field

[a] CNRS, LAAS-CNRS, 7, avenue du Colonel Roche BP 54200 31031 Toulouse cedex 4, France Tel: +33(0)5 61 33 62 59; E-mail: vmansard@laas.fr

† Electronic Supplementary Information (ESI) available: [details of any supplementary information available should be included here]. See DOI: 00.0000/00000000.

of polymer gel is gaining a new momentum in the last decade thanks to the development of tough gel[19–21] made of double network which are more adapted for mechanical application

We can find gels responding to various stimuli. Thermosensitive gels (e.g. polyNIPAM[22–24]) are simple to control by tuning the temperature. pH-sensitive (e.g. polyacrylic acid) or solvent-sensitive gels are more complex to control and require to change the surrounding solvent. Gels sensitive to simpler stimuli have been developed as gel sensitive to UV/visible light[25–28] or to magnetic field[16]. These external stimuli can modify the local temperature inside the gel, modify the chemical composition of the solvent or modify the polymer structure. Finally swelling and shrinking of gel can also be induced by applying a constant electric field[29,30] because of local modification of ion concentration by electropheresis.

Smart gels—as most of active materials—show isotropic swelling when we only require a displacement into a single dimension. Several strategies enable to convert this 3D-swelling into a directed displacement, which amplify actuator deformation or strength.

A first strategy consist on producing a composite material. For example thin film made of an active layer and an inert layer will bend when the active layer swells[16,18,31–34]. This design (and similar ones) are widely used with all types of active materials—especially with conductive polymer. It is particularly simple and it enables to amplify the movement. Small deformation of the active layer produces large bending of several centimeters. This design is particularly adapted for material with low swelling amplitude and when it is only possible to use thin layer.

Nevertheless, this design is poorly adapted for smart gel. Amplification of the movement necessarily goes with a reduction of the actuator strength. So thin film gel actuators are very weak because of this strength decrease combined with the low elastic modulus of gels. These actuators are only used as a proof of concept and for microactuation.

A better design would amplify the strength (even if it requires to reduce the displacement.) Recently, contracting fibers have been designed following this key idea. Active material is infiltrated into a spinned yarn[35–38]. When the active material swells, it twists the yarn and so the fibers contracts. A $50\,\mu$m diameter fiber can contract by 50 % (i.e. several centimeters) and lift about 0.1 N (which corresponds to 1000 times its own weight).

Artificial muscle can also be made of a gel sample inserted into a macroscopic system inspired by pneumatic soft robotics[39–41]. The gel act as the pressurized fluid for pneumatic muscle: when the gel swells, it applies a pressure on the walls of the soft muscle inducing its displacement. This strategy only work with smart gel because their particularly large swelling amplitudes.

Despite numerous strategies based on several type of active material, no artificial muscle have been efficiently used in a robot. To be used in robotics, a muscle has to fulfill two major requirements. First, artificial muscles must produce linear contraction as biological muscles. This is the only acceptable deformation for bioinspired robots. Unfortunately, linear contraction is more complex to produce than bending. Linear muscle requires active material with large deformation ratio of at least 20 to 30 %. Many active material are ruled out because of a low deformation ratio. At the opposite, smart gels—with very large swelling amplitude—are particularly adapted to tackle this challenge.

Secondly, we need a muscle big enough to produce large force and large displacement. Actuators with good normalized properties (e.g. displacement ratio) but with a small size are not adapted. Unfortunately, most actuators are made of thin layers of active material. They produce small displacements or are weak. Producing larger actuators with high volume of active material (instead of thin layers) is a challenging task. Such scale-up increases dramatically the response time of the actuators for all type of active material. Transport processes is, most of the time, the limiting kinetic factor. Indeed, actuation requires transfer of energy through the material (e.g heat transfer for thermoactive material...). Furthermore, materials with large swelling amplitude (conductive polymers and smart gels) require a mass transfer for swelling (transfer of ions for conductive polymers and diffusion of solvent for smart gels). Increasing the quantity of active material slows down transfer and therefore increases the response time. One overcame this limit by stacking many "small" actuators[42,43] together but this strategy highly increases the complexity of the final muscle.

The challenge today is to synthesize an active material with large deformation ratio where response time is not degraded when using large sample. In this article, we present a strategy overcoming these limitations. Our material is based on a pH-sensitive smart gel, the poly-acrylic acid gel (pAA)[44]. Gel swelling kinetic is limited by the transport of solvent through the gel by diffusion[45]. The diffusion coefficient[45–47] is typically about 10^{-11} to $10^{-10}\,\mathrm{m^2/s}$ and swelling time below 1 s would only be possible for system with a size below $10\,\mu$m. To accelerate the swelling, we suggest to synthesize gels with a macroporous structure with holes of about $100\,\mu$m. This is a key idea of this article. It has been demonstrated that porous gel swell faster[48–50]. The porosity vascularize the gel and enable fast transport of solvent by convection. Macroporous gel are commmonly used in tissue engineering[51–53] drug delivery[54,55].

Many strategies are described in the literature to produce macroporous gel. Superporous hydrogel[56,57] are obtain by adding porogen—as calcium carbonate—which create pores during polymerization. Macropores can be created by using a template before crosslinking. The template can be made of an emulsion[58,59], a foam[60,61], or solid sacrificial particles[50,53]. Adding porosity often weaken the gel but He et al.[22,62] demonstrated that porous gel can also show enhanced mechanical properties using freezecasting or cononsolvent techniques.

Only few prototypes of muscle integrate a porous material[39–41,48,63,64]. Tondu et al.[40,41] built a muscle with large size and high strength based on porous gel. The muscle is a cylinder of 100 mm by 8 mm. It can contract by 20 mm and can lift a very high force of 60 N. The porous active part is made of packed gel beads with a diameter of 1 mm. The reaction time is highly reduced compared to the use of non-porous gel but remain very long—about 1 h. This slow reaction time is mostly due to the size of the gel beads, which are too large for fast actuation. He el al.[63] made a muscle based on porous liquid crystal elastomer. The porosity

is used to accelerate the heat transfer by convection. The muscle can contract by 20 mm and lift 1 N with a reaction time below 10 s.

Adding porosity for accelerating transport processes is commonly used in chemical engineering. Nevertheless the development of a porous active material raises specific questions. The mechanical aspects have to be considered. A compromise has to be found between fast transport and high strength. In this article we demonstrate that our material offer a good enough compromise. We first study the mechanical aspect of the porous material. We then characterize the swelling speed and demonstrate the porosity highly decrease the response time. Finally, we demonstrate that this material can be used into an artificial muscle with linear contraction.

1 Material and methods

Synthesis of macroporous gel

All the chemicals are provided by sigma aldrich and used as received : acrylic acid (AA) (CAS #79-10-7); N,N'-Methylenebisacrylamide (Baam)(CAS #110-26-9) and Irgacure 651 (CAS #24650-42-8).

The pH-sensitive polyacrylic acid (pAA) gel is reticulated under UV from an aqueous solution of monomer. The monomer solution is composed of AA as monomer (concentration 2.8 mol/L), Baam as crosslinker (concentration ranging from $1\%_{\text{mol}}$ to $5\%_{\text{mol}}$— 2.8×10^{-2} to 1.4×10^{-1} mol/L) and Irgacure 651 as UV-sensitive activator (concentration $0.07\%_{\text{mol}}$—2×10^{-3} mol/L). The variation of the crosslinker concentration modifies the gel elasticity and swelling ratio.

The gel can be reticulated as it is—designated as *bulk gel*—or with a macroporous structure—designated as *macroporous gel (MPgel)*. To produce MPgels, we reticulate the gel around a template which is then removed[53]. The template is made of PMMA particles (colacryl 3000, Lucite international) with a diameter 100 μm. Particles are first packed into a mold ($\varnothing\times$ height 7.5×10.5 mm) and sintered at 185 °C for 6 h. Sintering is a key step which ensure the pores to be open and connected in order to allow easy flow through the gel. The template is filled by the monomer solution by dipping it into the solution and leaving it under vacuum for 6 h to remove trapped bubbles. The gel is then reticulated under UV for 20 min. The template is dissolved by three successive 24h-baths of ethyl acetate under mild mixing. The gel is finally rinsed into successive 24h-baths of first ethanol and then sodium phosphate buffer (0.1 mol/L) at pH = 2 or pH = 10. In this article the pH of the gel will be switched using the two buffer solutions (H_3PO_4@0.1 mol/L pH=2 or $NaPO_4$@0.1 mol/L pH=10). We add a pH indicator to visualize the pH (*bromocresol green* with a transition at pH=5).

hydraulic system and McKibben muscle

We build an hydraulic system to switch the gel pH by convection and to obtain fast swelling. The system is made of a cylinder of MPgel with $[\text{Bamm}] = 3\%_{\text{mol}}$ ($\varnothing\times$height: 7.5×11.5 mm@pH= 2 — 11.5×17.8 mm@pH= 10) inserted into a silicon rubber tube (ecoflex 0030, inner$\varnothing$: 6 mm; outer$\varnothing$: 10 mm). The inlet and outlet are 3Dprinted.

We control the flow rate the buffer is inject. To do so, we inject the fluid at controlled pressure and we use a long tubing, which creates high hydraulic resistance upstream of the MPgel. The flow rate is measured by weight using a precision scale. An electrovalve enable to switch quickly the type of buffer we are injecting (Masterflex Biochem Valve 080T324-62). The pressure drop due to gel is measured as close as possible to the gel sample using a pressure sensor (Honeywell pressure sensor HSC series—#HSCDRRN100MDSA3). We check that we measure a negligible pressure drop without the gel sample inserted into the system. All the electronic equipment are controlled using an Arduino microcontroller.

To obtain a muscle with linear constraction we build a braid made of nylon wire ($\varnothing$0.2 mm) as for pneumatic McKibben muscle. This braid convert radial swelling in contraction.

2 Mechanical properties at equilibrium

MPgels have the microscopic porous structure [Fig.1b] of a solid foam[65–67]. It is constituted of spherical cavities with a diameter of 100 μm to 150 μm well connected through holes of 30 μm. The microstructure reproduces well the shape imposed by the initial PMMA particle template. Therefore the porosity—i.e. void fraction—has to be close to the initial particle fraction and can be estimated about $\rho = 60\,\%$.

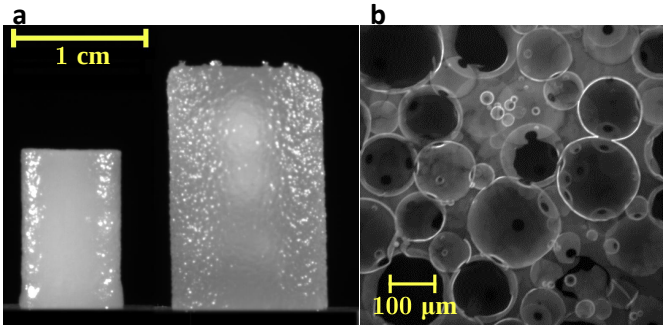

Fig. 1 (a) Picture of MPgel with $[\text{Baam}] = 3\%_{\text{mol}}$ in the unswollen (pH = 2) and swollen (pH = 10) state. (b) Picture of MPgel by confocal microscopy averaged over a depth of 50 μm.

When we increase the pH by changing the surrounding buffer solution, both porous and bulk gels swell reversibly with a pH transition of about pH=5 [Fig.1a & 2a]. This swelling is due to the ionization of the carboxilic site which induce a transition from globule to coil[68]. We measure the swelling ratio $\Gamma = V_{\text{base}}/V_{\text{acid}}$ [Fig.2b] —where the V_{acid} and V_{base} are the gel volume at, respectively, pH = 2 and pH = 10. As expected, pAA gels present a very large swelling ratio. The volume can be multiplied by up to 7 times and even at high crosslinker concentration, the swelling ratio is above 2.5. MPgels present a lower swelling ratio than bulk gels with $\Gamma_{\text{porous}} \approx 0.8\cdot\Gamma_{\text{bulk}}$. We will come back on this difference during the discussion on the elastic modulus.

We characterize the mechanical properties of both bulk gels and MPgels using uniaxial compression test [Fig.3a]. The characterization is systematically performed over at least 3 samples and only small deviations are observed. Bulk gel present a typical response of fragile material with a linear response at low

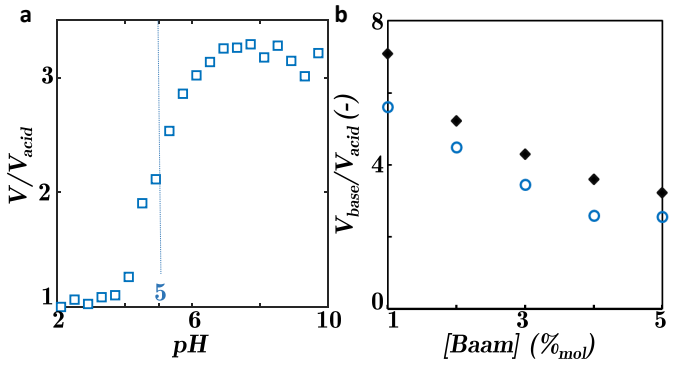

Fig. 2 (a) Example of the variation of volume of a gel sample as function of the pH (MPgels with [Baam] = 3 %mol) (b) Swelling ratio $\Gamma = V_{\text{base}}/V_{\text{acide}}$ for (blue) MPgels and (black) bulk gels.

strain and a breaking at strain above 30 to 50 %. The deformability (i.e. maximum strain) decrease with the crosslinker concentration and when the gel is swollen (high pH). For MPgels, the stress-strain curves have the typical shape of cellular materials[67]. Three regimes can be identified: the linear elastic response at low strain ($\varepsilon < 10\%$), a plateau—called *elastic bukling*—for $\varepsilon < 40\%$, and finally the densification regime where the stress diverges at high strain.

MPgels with low cross linker concentration ([Baam] $\leq 3\,\%_{\text{mol}}$) are much more deformable than bulk gel. MPgels can be compressed up to 70 % without breaking and they can sustained several compression cycles without degradation [inset Fig.3a]. The increase in robustness is unexpected. Usually, porous media are more fragile than the bulk material they are made of. MPgels with [Baam] $\geq 4\,\%_{\text{mol}}$ are also more deformable at low pH but when they are swollen—conditions of highest fragility for bulk gels—they become very fragile and break at small strain ($\sim 10\%$).

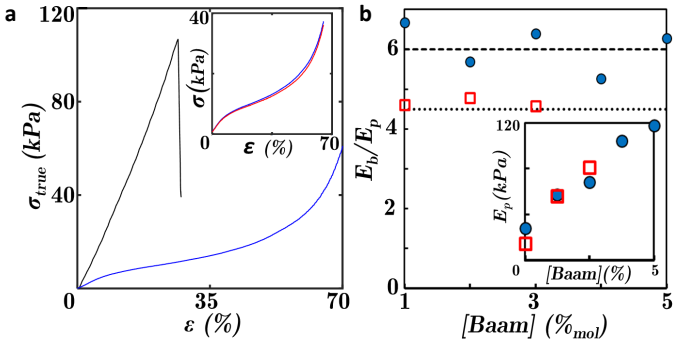

Fig. 3 (a) Compression curve for MPgel (blue) and bulk gel (black) at [Baam] = 3%mol. (inset) Compression curve of MPgel after 1 (blue) and 10 (red) compression cycle at $\varepsilon = 65\%$. (b) Ratio E_b/E_p between Young modulus of bulk gels and of MPgels as function the crosslinker concentration in (blue) unswollen/acide and (red) swollen/basic state. (inset) Young modulus of MPgels E_p as function of the crosslinker concentration.

As expected, MPgels show a lower compressive stress than bulk gel. Adding porosity always weaken the materials. From the initial linear response, we estimate the Young modulus E_p and E_b of, respectively, MPgels and bulk gels. The ratio of modulus E_b/E_p is found independent on the cross linker concentration [Fig.3b]. We measure $E_b/E_p = 6 \pm 0.5$ in the unswollen/acid state and $E_b/E_p = 4.5 \pm 0.2$ in the swollen/basic state.

The modulus ratio is expected to be independent of the bulk material properties but to depend only on the porous structure. For solid foams with open cells, the ratio is only a function of the porosity ρ [67]:

$$\frac{E_b}{E_p} = \frac{1}{(1-\rho)^2} \tag{1}$$

Therefore, we can deduce that the porous structure is independent on the crosslinker concentration with a porosity $\rho_{\text{acid}} = 60\%$ in the unswollen state and $\rho_{\text{base}} = 53\%$ in the swollen state. This result indicates that the swelling is not homothetic. During swelling, the pores get smaller and MPgels become less porous.

This reduction of porosity is consistent with our previous observation on the swelling ratio $\Gamma_{\text{porous}} \approx 0.8 \cdot \Gamma_{\text{bulk}}$. Let's suppose that the walls of MPgels swell with the same amplitude than bulk gel. Part of this swelling induces deformation of MPgels at macroscopic scale. Another part induces a reduction of the porosity. Conservation of the volume gives a relation between porosity at low and high pH:

$$1 - \rho_{\text{base}} = \frac{\Gamma_{\text{bulk}}}{\Gamma_{\text{porous}}}(1 - \rho_{\text{acid}}) \tag{2}$$

The swelling ratio measurement would then implicate that the porosity decreases from $\rho_{\text{acid}} = 60\%$ to $\rho_{\text{base}} = 50\%$— which is consistent with our previous estimations.

Active materials, as MPgels, need to produce mechanical effort during swelling. So it is not sufficient to characterize them after they swell freely. We also measure the pressure σ_{swell} that MPgels apply when they swell under constrain [Fig.4a]. A cylinder of unswollen MPgels is placed in a beaker between two fixed plates. We change the buffer surrounding the gel in order to swell it. The pH inside the gel increases slowly by diffusion. We measure the force the gel applies on the top plate. The pressure force increases slowly and reaches a plateau F_{swell} after ~ 12 h. The swelling presssure is defined as $\sigma_{\text{swell}} = F_{\text{swell}}/S$, where S the final section of the gel cylinder. σ_{swell} increases with the crosslinker concentration [Fig.4c]. MPgel with higher crosslinker concentration swells with a lower amplitude but produces higher force. MPgels can apply a pressure of 15 kPa (150 mbar). This is sufficient for an efficient actuation and many soft pneumatic robots are actuated with similar pressure[3,5].

It is also important to notice that swelling under constrain does not impact the final properties of MPgels. Constrained-swollen MPgels show the same compression curve than freely-swollen ones. Furthermore, the swelling stress σ_{swell} is directly related to the mechanical behavior measured after swelling. Indeed, we measure the stress σ_{comp} [Fig.4b] required to compress a freely-swollen MPgel from a height L_{base} to L_{acid}, i.e. to a strain $\varepsilon_{\text{comp}} = (L_{\text{base}} - L_{\text{acid}})/L_{\text{base}}$. We observe a good agreement between σ_{swell} and σ_{comp}.

3 Swelling kinetic

We now study the swelling kinetic and we will demonstrate that MPgels can swell in 100 s. In the previous section, sample takes hours to swell because the pH was switched only using molecular

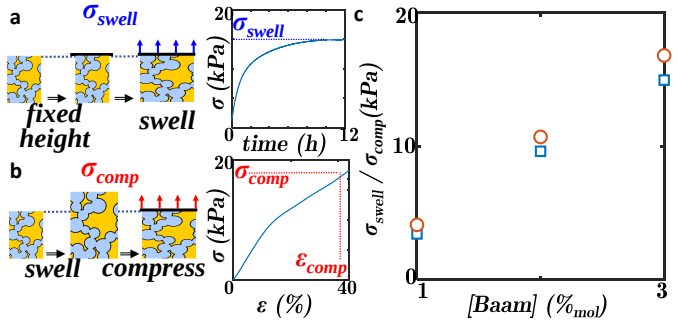

Fig. 4 (a-b) Illustration on how σ_{swell} and σ_{comp} are measured. (a) The swelling stress σ_{swell} corresponds to pressure applied by the gel when the pH is changed but the gel is maintained at constant height. (b) σ_{comp} correspond to the stress required to compress a freely-swollen gel back to its initial height L_{acid}. On the right, we show where we read σ_{comp} on the compression curve (c) (blue) σ_{swell} and (red) σ_{comp} as function of the crosslinker concentration. We found a good agreement between both stresses.

diffusion. The swelling speed is dramatically increased when the pH is switch by convection. To do so, we developped a fluidic system, which enables to flow buffer solutions through a cylinder of MPgel, while letting it swell freely. The system is made of a cylinder of MPgel inserted into a flexible silicone rubber tube (ecoflex 0030) [Fig.5a&b]. The inner tube diameter is chosen slightly smaller than the gel sample in order to maintain the sample in the middle of the tube and to flow the buffer through the gel and not around it. Buffer at high or low pH is injected at controlled flow rate and we use use an electrovalve to switch quickly—within less than 5s—the type of buffer we are injecting. The evolution of the pH is observed thanks to a pH indicator (*bromocresol green* with a transition at pH = 5).

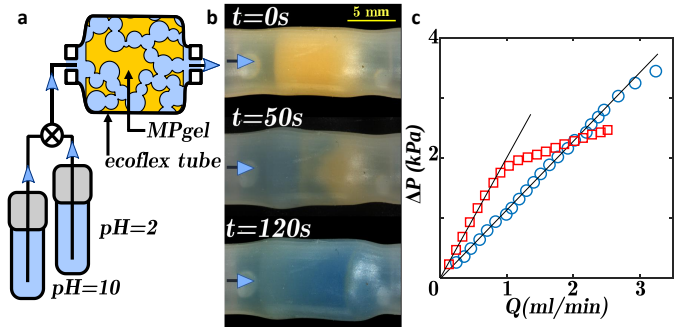

Fig. 5 (a) Schematic of the device to change quickly the pH by convection. A cylinder of MPgel is inserted into a flexible tube. Buffer solution at low and high pH are injected at controled flow rate. An electrovalve enable to switch quickly between both solution. (b) Picture of the swelling of MPgel at different times when we flow a basic buffer from left to right. A color indicator shows the pH (yellow $pH < 5$ and blue $pH > 5$) (c) Pressure drop as function of the flow rate for MPgel in (blue) acid state and (red) basic state. The linearity at small flow rate is in good agreement with the Darcy's law.

By injecting buffer solution, the gel swells reversibly and dilate the rubber tube, which is chosen flexible enough to have small impact of the gel swelling. Indeed, the tube behaves as a rubber balloon[69]. Under low hydrostatic pressure, the tube remain nearly unchanged but above a critical pressure—about 5 kPa—it inflates. Therefore it applies a radial stress of about 5 kPa on the MPgel sample when swelling—which is lower than $\sigma_{swell} = 15$ kPa. Nevertheless, the impact of the tube is not negligeable. When swelling, the diameter of the tube only increases by 20 % (from 11.5 mm to 13.7 mm), when the diameter of free gel increases by 50 % (from 7.5 mm to 11.5 mm). This reduction of amplitude has two causes. The measured diameter also include the rubber walls (with a thickness of 2×2 mm), which do not swell. Furthermore the tube limit the swelling of the gel cylinder. The diameter of swollen gel inside the tube is about 10 mm (vs. 11.3 mm for free gels).

We measured the hydraulic pressure drop ΔP for gels at equilibrium when we flow the buffer solution through [Fig.5c]. At low flow rate, we observe a good linearity between ΔP and the flow rate Q, which is in good agreement with the Darcy's law. The permeability (defined as $k = \mu LQ/S\Delta P$ where μ is the water viscosity, L and S the length and section of the gel sample) is equal to $k = 4 \times 10^{-12}$ m^2 for unswollen gel and $k = 2 \times 10^{-12}$ m^2 for swollen gel. At higher flow rate, we lost the linearity and the system behave as if the permeability was increased. It is likely due to a very small inflation of the tube. The buffer is then allowed buffer to partially flow on the side of the gel. In the following we will work with flow rate below 4 mL/min ($\Delta P < 5$ mbar). The tube is not inflated at this pressure and it is important to emphasize that *the inflation is not due to the hydraulic pressure but to the gel.*

We can already notice that a compromise has to be made on the flexibility of the rubber tube. Using a more flexible and thinner tube would allow larger swelling. Nevertheless a more flexible tube would be limited to lower flow rates. We will see later that this rubber tube is one of the major drawback of our system.

We observe a quick swelling of the gel sample in 100 to 200 s, when we switch buffer solutions from low to high pH,. We measure the evolution of tube diameter [Fig.6] using simple image analysis developed on Matlab for different flow rate from 0.5 to 4 mL/min. MPgel swells faster when we increase the flow rate. To understand what control the kinetic, we plot the diameter as function of the volume of injected buffer solution V_{inj} [Fig.6b]. All the curves collapse onto a masters curve. The gel is fully swollen

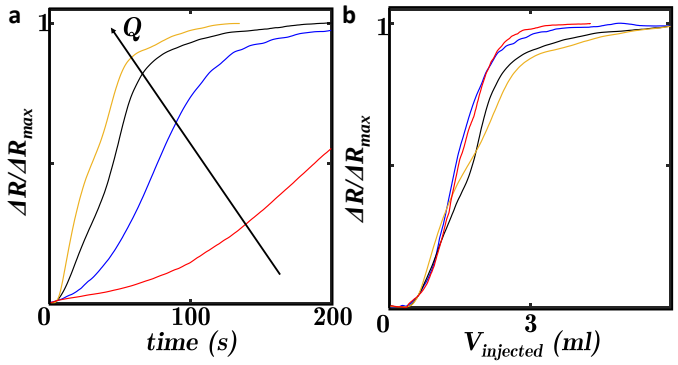

Fig. 6 (a-b) Relative variation of the diameter $\Delta R/\Delta R_{max}$ as function of (a) time and (b) volume of buffer $V_{injected}$ for different flow rate $Q = 0.52$, 1.06 , 2.5 , 3.9 mL/min.

after we injected 4 mL. It corresponds to a quantity of Na_3PO_4 of 300 μmol—for comparison the quantity of acrylic site in the gel cylinder is about 500 μmol. In conclusion, the swelling kinetic is controlled by the volume of buffer solution injected and the convection is the limiting kinetic process. By improving this process, we could accelerate MPgel swelling. The exact comprehension the swelling kinetics and the modelization of the transport through the gel is left for future work.

4 Artificial muscle

We finally demonstrate that MPgel can be efficiently used for building an artificial muscle. The challenge is to develop a mechanical structure, which convert the swelling into an actuation. MPgels are designed to have a very large swelling ratio so they can be integrated into a muscle inspired by pneumatic soft actuators. More specifically, we build a muscle based on the McKibben muscle[6,70,71]. This muscle present several key advantages. It is simple to build and produce linear contraction well adapted for robotics.

The muscle is made of a cylinder of MPgel inserted into an ecoflex tube as in the previous section. The tube is—now— surrounded by a double-helix-braided sheath made of inextensible nylon wires [Fig7]. This sheath convert the swelling into linear contraction: when swelling, the gel pushes radially on the braided sheath and induces an axial contraction. The muscle is composed of a 22 mm long active part and two inlet of 25 m. The active part, includes the gel cylinder (10 mm long at low pH) and enough space to allow swelling of the gel and contraction of the muscle.

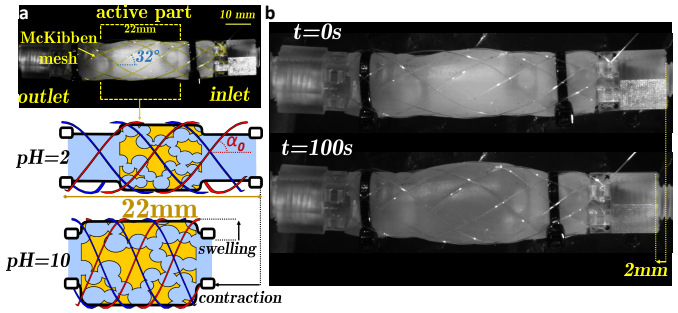

Fig. 7 (a) Picture and schematic of the McKibben gel muscle. The muscle is made of a cylinder of MPgel in a rubber tube. A braid of inextensible nylon wires (highlighted in yellow) convert the swelling into contraction. (b) Picture of the contraction of the muscle when we flow a basic buffer solution.

When we flow high pH buffer, the gel swell quickly and the muscle contracts. When no load is applied on the muscle, the displacement is $\Delta L = 2$ mm, which is about 9 % of the active part. In isostatic configuration—where the muscle is not allowed to move—we measure a force of 1.5 N (corresponding to a weight of 150 g).

The behavior of the McKibben muscle is well understood. The inextensible braid imposes a relation between the contraction and the diameter of the muscle[70]:

$$\Delta L_{\text{theory}} = L_0 \left(1 - \frac{1}{\cos \alpha_0} \sqrt{1 - \frac{r_{\text{base}}}{r_{\text{acid}}} \sin^2 \alpha_0} \right) \tag{3}$$

where $\alpha_0 = 32°$ is the angle of the McKibben braid (as defined in Fig.7a), $r_{\text{acid}} = 10$ mm and $r_{\text{base}} = 12.5$ mm are the muscle diameters in both configuration and $L_0 = 22$ mm the muscle length which is taken equal to the length of the active part. The model predict a contraction of $\Delta L_{\text{theory}} = 4$ mm. The measured displacement is actually smaller because the rubber tube does not allow an homogenous swelling. The edge are sligtly thinner. We also notice that without the limit of the rubber tube, we would have $r_{\text{base}}/r_{\text{acid}} = 150\,\%$ and a much larger displacement of $\Delta L_{\max} = 7$ mm.

On an other hand, if the gel apply an homogeneous radial stress σ_r, the model predicts a force under zero displacement equal to*:

$$F_{\text{theory}} = \frac{\pi . r_{\text{acide}}^2}{2 \tan^2 \alpha_0} \sigma_r \tag{4}$$

If we suppose $\sigma_r = \sigma_{\text{swell}} = 15$ kPa, we should get $F_{\text{theory}} = 6.6$ N, which is 4 times higher than what is measured. The lower measured force is probably due to the rubber tube, which imposed constrain on the gel and reduces the pressure applied on the McKibben mesh.

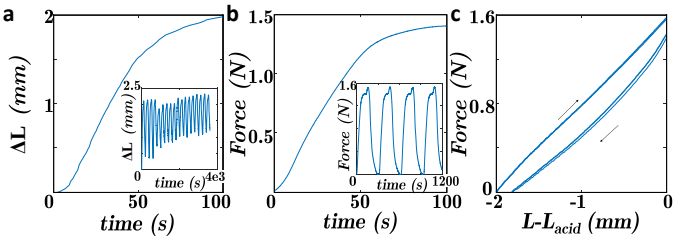

Fig. 8 (a-b) characterization of the response of the muscle with time when we flow $pH = 10$ buffer solution at $Q = 3.9$ mL/min (a) Variation of the muscle length ΔL when no load is applied to the muscle. (inset) Evolution of ΔL when submitted to base/acid cycles. (b) Force produced by the muscle under isostatic configuration. (inset) Evolution of the force when submitted to bases/cycles. (c) Force as function of the elongation when we pull on a muscle after reaching equilibrium in the basic/contracted state. We plot 3 cycles of elongation. The measurement shows hysteresis due to solid friction but no degradation of the muscle.

The muscle contracts in 100 s [Fig.8] with the same kinetic as observed in the previous section and supports many cycle of contraction. However, we observe a reduction of amplitude of contraction during cycling [inset Fig.8a]. It is not due to a degradation of the muscle but due to solid friction in the mesh, which create hysteresis (as observed also for pneumatic McKibben muscle.) When the muscle is gently manipulated to realign the mesh, the initial properties of the muscle are recovered. Furthermore no degradation of the force is observed for cycle under isostatic condition[inset Fig.8b]. This hysteresis is also visible when we measure the force as function of the elongation for the swollen (i.e. basic) muscle [Fig.8c].

*equation adapted from[70] with considering only the radial pressure.

5 Discussion

In this article, we present an new promising active material, which show fast swelling even at large volume. This is possible because we added porosity to the material. Up to now, active material were limited by transport phenomena and could not be used at large enough volume. Using porous media is commonly used in chemical engineering to facilitate transport. Porous active material is—in our opinion—one of the only sensible strategy to increase the volume used while keeping a high-enough actuation speed. We believe that this article represent an important step toward this direction.

We observed an important reduction of the swelling time–from several hours or days for bulk gel to few minutes for MPgel. MPgels are unfortunately still too slow for robotics. Nevertheless, it is particularly interesting that the swelling speed is no more limited by solvent diffusion but controlled by the time to switch pH.

Switching the pH by convection is complex as it requires pump and tubing. Switching by convection is also slow. So the speed of the muscle is still not sufficient for impactful applications. Robots would require a contraction time below $1\,\mathrm{s}$. To accelerate the swelling, we would have to develop MPgels with a simpler way to control the swelling as thermosensitive gels (e.g. pNIPAM)[24,72], or light sensitive gel[27,73] or gel controlled by electrochemistry[74]. The macroporosity would still be key to accelerate the transport of solvent and to enable fast swelling. Macroporous gel with such capacities will be faster to react and easier to integratelead to a muscle simple to integrate and fast enough to be used in robotics.

The porosity also impacts the mechanical properties of MPgel. It reduces MPgel modulus and the force produced while swelling. In this articles we used a template of spherical particles, which have to be in close contact to ensure the pores to be connected. This process imposes a large porosity of $60\,\%$, which divide the modulus by 5 MPgels still produce a pressure $\sigma_{\mathrm{swell}} = 15\,\mathrm{kPa}$ sufficient for soft robotic. To go further and to improve the force produced during swelling we would have to synthesis gel with a lower porosity, while keeping the pores connected. We could used a template made of fibers[50] instead of spherical particles. The recent development of porous gel based on bicontinuous emulsion (bijels) also represent another interesting strategy[75,76].

Finally, we showed that the porosity also highly improves MPgels robustness It is a significant and unexpected advantage. The gel cylinder is the most fragile component of our muscle but we still obtain a robust muscle, which can stand many cycles. However, our system could highly benefit from the recent and very active research on "tough gel"[19–21]—where the robustness is improved thanks to a double polymer network.

Acknowledgment

This work was supported by LAAS-CNRs micro and nanotechnology platform , a member of the Renatech french national network.

Notes and references

1 A. Carpentier, C. Latrémouille, B. Cholley, D. M. Smadja, J. C. Roussel, E. Boissier, J. N. Trochu, J. P. Gueffet, M. Treillot, P. Bizouarn, D. Méléard, M. F. Boughenou, O. Ponzio, M. Grimmé, A. Capel, P. Jansen, A. Hagège, M. Desnos, J. N. Fabiani and D. Duveau, *The Lancet*, 2015, **386**, 1556–1563.

2 J. D. Madden, *Science*, 2007, **318**, 1094–1097.

3 F. Ilievski, A. D. Mazzeo, R. F. Shepherd, X. Chen and G. M. Whitesides, *Angewandte Chemie - International Edition*, 2011, **50**, 1890–1895.

4 B. Gorissen, D. Reynaerts, S. Konishi, K. Yoshida, J.-W. W. Kim and M. De Volder, *Advanced Materials*, 2017, **29**, 1604977.

5 F. Connolly, C. J. Walsh and K. Bertoldi, *Proceedings of the National Academy of Sciences*, 2016, **114**, 201615140.

6 B. Tondu and P. Lopez, *Control Systems, IEEE*, 2000, 15–38.

7 K. J. De Laurentis and C. Mavroidis, *Technology and Health Care*, 2002, **10**, 91–106.

8 K. K. Safak and G. G. Adams, *Robotics and Autonomous Systems*, 2002, **41**, 225–243.

9 C. Ohm, M. Brehmer and R. Zentel, *Advanced Materials*, 2010, **22**, 3366–3387.

10 O. M. Wani, H. Zeng and A. Priimagi, *Nature Communications*, 2017, **8**, 1–7.

11 *Electromechanically Active Polymers a concise reference*, ed. F. Carpi, Springer, 2016.

12 L. Ionov, *Materials Today*, 2014, **17**, 494–503.

13 S.-K. Ahn, R. M. Kasi, S.-C. Kim, N. Sharma and Y. Zhou, *Soft Matter*, 2008, **4**, 1151.

14 A. Baldi, Y. Gu, P. E. Loftness, R. A. Siegel and B. Ziaie, *Journal of Microelectromechanical Systems*, 2003, **12**, 613–621.

15 R. Yoshida, T. Sakai, Y. Hara, S. Maeda, S. Hashimoto, D. Suzuki and Y. Murase, *Journal of Controlled Release*, 2009, **140**, 186–193.

16 J. C. Breger, C. Yoon, R. Xiao, H. R. Kwag, M. O. Wang, J. P. Fisher, T. D. Nguyen and D. H. Gracias, *ACS Applied Materials and Interfaces*, 2015, **7**, 3398–3405.

17 L. Dong and H. Jiang, *Soft Matter*, 2007, **3**, 1223.

18 W. J. Zheng, N. An, J. H. Yang, J. Zhou and Y. M. Chen, *ACS Applied Materials and Interfaces*, 2015, **7**, 1758–1764.

19 J. P. Gong, Y. Katsuyama, T. Kurokawa and Y. Osada, *Advanced Materials*, 2003, **15**, 1155–1158.

20 Y. Chen, X. Liu and Y. Zhao, *Applied Physics Letters*, 2015, **106**, 141601.

21 S. Naficy, G. M. Spinks and G. G. Wallace, *ACS Applied Materials and Interfaces*, 2014, **6**, 4109–4114.

22 Y. Alsaid, S. Wu, D. Wu, Y. Du, L. Shi, R. Khodambashi, R. Rico, M. Hua, Y. Yan, Y. Zhao, D. Aukes and X. He, *Advanced Materials*, 2021, **33**, 1–9.

23 K. Haraguchi, T. Takehisa and S. Fan, *Macromolecules*, 2002, **35**, 10162–10171.

24 M. A. Haq, Y. Su and D. Wang, *Materials Science and Engineering C*, 2017, **70**, 842–855.

25 J. E. Stumpel, D. Liu, D. J. Broer and A. P. H. J. Schenning, *Chemistry - A European Journal*, 2013, **19**, 10922–10927.

26 A. Suzuki, T. Ishii and Y. Maruyama, *Journal of Applied Physics*, 1996, **80**, 131–136.

27 T. Tatsuma, K. Takada and T. Miyazaki, *Advanced Materials*, 2007, **19**, 1249–1251.

28 Y. Takashima, S. Hatanaka, M. Otsubo, M. Nakahata, T. Kakuta, A. Hashidzume, H. Yamaguchi and A. Harada, *Nature Communications*, 2012, **3**, 1270–1278.

29 Tanaka, *Science*, 1982, 467–469.

30 D. Morales, E. Palleau, M. D. Dickey and O. D. Velev, *Soft Matter*, 2014, **10**, 1337–1348.

31 F. M. Cheng, H. X. Chen and H. D. Li, *Journal of Materials Chemistry B*, 2021, **9**, 1762–1780.

32 G. Stoychev, N. Puretskiy and L. Ionov, *Soft Matter*, 2011, **7**, 3277–3279.

33 J. Kim, J. A. Hanna, R. C. Hayward and C. D. Santangelo, *Soft Matter*, 2012, **8**, 2375–2381.

34 J. Kim, J. A. Hanna, M. Byun, C. D. Santangelo and R. C. Hayward, *Science*, 2012, **335**, 1201–1205.

35 C. S. Haines, M. D. M. Lima, N. Li, G. M. Spinks, J. Foroughi, J. D. Madden, S. H. S. J. Kim, S. Fang, M. J. De Andrade, F. Göktepe, Ö. Göktepe, S. M. Mirvakili, S. Naficy, X. Lepró, J. Oh, M. E. Kozlov, S. H. S. J. Kim, X. Xu, B. J. Swedlove, G. G. Wallace and R. H. Baughman, *Science*, 2014, **343**, 868–872.

36 M. D. M. Lima, N. Li, M. J. De Andrade, S. Fang, J. Oh, G. M. Spinks, M. E. Kozlov, C. S. Haines, D. Suh, J. Foroughi, S. J. Kim, Y. Chen, T. Ware, M. K. Shin, L. D. Machado, A. F. Fonseca, J. D. Madden, W. E. Voit, D. S. Galvão, R. H. Baughman, M. D. Andrade and S. Fang, *Science*, 2012, **338**, 928.

37 A. Maziz, A. Concas, A. Khaldi, J. Stålhand, N. K. Persson and E. W. Jager, *Science Advances*, 2017, **3**, 1–12.

38 M. Kanik, S. Orguc, G. Varnavides, J. Kim, T. Benavides, D. Gonzalez, T. Akintilo, C. C. Tasan, A. P. Chandrakasan, Y. Fink and P. Anikeeva, *Science (New York, N.Y.)*, 2019, **365**, 145–150.

39 B. Salahuddin, H. Warren and G. M. Spinks, *Smart Materials and Structures*, 2020, **29**, year.

40 B. Tondu, S. Mathé and R. Emirkhanian, *Sensors and Actuators A: Physical*, 2010, **159**, 73–78.

41 B. Tondu, R. Emirkhanian, S. Mathé and a. Ricard, *Sensors and Actuators A: Physical*, 2009, **150**, 124–130.

42 F. Carpi, C. Salaris and D. De Rossi, *Smart Materials and Structures*, 2007, **16**, s300–s305.

43 T. Hwang, Z. Frank, J. Neubauer and K. J. Kim, *Scientific Reports*, 2019, **9**, 2–10.

44 O. E. Philippova, D. Hourdet, R. Audebert and A. R. Khokhlov, *Macromolecules*, 1997, **30**, 8278–8285.

45 J. Yoon, S. Cai, Z. Suo and R. C. Hayward, *Soft Matter*, 2010, **6**, 6004.

46 T. Tanaka and D. J. Fillmore, *The Journal of Chemical Physics*, 1979, **70**, 1214.

47 M. Quesada-Pérez, J. A. Maroto-Centeno, J. Forcada and R. Hidalgo-Alvarez, *Soft Matter*, 2011, **7**, 10536.

48 M. L. O'Grady, P. L. Kuo and K. K. Parker, *ACS Applied Materials and Interfaces*, 2010, **2**, 343–346.

49 B. Ziółkowski, L. Florea, J. Theobald, F. Benito-Lopez and D. Diamond, *Journal of Materials Science*, 2016, **51**, 1392–1399.

50 H. Warren, D. J. Shepherd, M. in het Panhuis, D. L. Officer and G. M. Spinks, *Sensors and Actuators, A: Physical*, 2020, **301**, 111784.

51 L. Ren, K. Tsuru, S. Hayakawa and A. Osaka, *Biomaterials*, 2002, **23**, 4765–4773.

52 S. J. Bryant, J. L. Cuy, K. D. Hauch and B. D. Ratner, *Biomaterials*, 2007, **28**, 2978–2986.

53 R. B. Diego, M. P. Olmedilla, Á. S. Aroca, J. L. Ribelles, M. M. Pradas, G. G. Ferrer and M. S. Sánchez, *Journal of Materials Science*, 2005, **40**, 4881–4887.

54 Y. Wen, Y. Liu, H. Zhang, M. Zou, D. Yan, D. Chen and Y. Zhao, *Nanoscale*, 2019, **11**, 2687–2693.

55 Z. Ayar, M. Shafieian, N. Mahmoodi, O. Sabzevari and Z. Hassannejad, *Journal of Applied Polymer Science*, 2021.

56 H. Omidian, J. G. Rocca and K. Park, *Journal of controlled release*, 2005, **102**, 3–12.

57 K. Kabiri, H. Omidian and M. J. Zohuriaan-Mehr, *Polymer International*, 2003, **52**, 1158–1164.

58 M. S. Silverstein, O. Kulygin and M. S. Silverstein, *Soft Matter*, 2007, **3**, 1525.

59 P. Krajnc, D. Štefanec and I. Pulko, *Macromolecular Rapid Communications*, 2005, **26**, 1289–1293.

60 W. Busby, N. R. Cameron and C. A. B. Jahoda, *Biomacromolecules*, 2001, **2**, 154–164.

61 A. Barbetta, G. Rizzitelli, R. Bedini, R. Pecci and M. Dentini, *Soft Matter*, 2010, **6**, 1785.

62 M. Hua, S. Wu, Y. Ma, Y. Zhao, Z. Chen, I. Frenkel, J. Strzalka, H. Zhou, X. Zhu and X. He, *Nature*, 2021, **590**, 594–599.

63 Q. He, Z. Wang, Z. Song and S. Cai, *Advanced Materials Technologies*, 2019, **4**, 1–7.

64 R. Luo, J. Wu, N.-D. Dinh and C.-H. Chen, *Advanced Functional Materials*, 2015, **25**, 7272–7279.

65 A. M. Kraynik, *MRS Bulletin*, 2003, **28**, 275–278.

66 A. Barbetta and N. R. Cameron, *Macromolecules*, 2004, **37**, 3188–3201.

67 L. J. Gibson and M. F. Ashby, *Cellular solids: Structure and properties, second edition*, Cambridge University Press, Cambridge, 2014, pp. 1–510.

68 T. Swift, L. Swanson, M. Geoghegan and S. Rimmer, *Soft Matter*, 2016, **12**, 2542–2549.

69 R. Mangan and M. Destrade, *International Journal of Non-Linear Mechanics*, 2015, **68**, 52–58.

70 B. Tondu, *Journal of Intelligent Material Systems and Structures*, 2012, **23**, 225–253.

71 F. Daerden and D. Lefeber, *European Journal of Mechanical and Environmental Engineering*, 2002, **47**, 11–21.

72 E. S. Gil and S. M. Hudson, *Biomacromolecules*, 2007, **8**, 258–264.

73 Z. Shi, P. Peng, D. Strohecker and Y. Liao, *Journal of the American Chemical Society*, 2011, **133**, 14699–14703.

74 K. Takada, N. Tanaka and T. Tatsuma, *Journal of Electroanalytical Chemistry*, 2005, **585**, 120–127.

75 M. F. Haase, H. Jeon, N. Hough, J. H. Kim, K. J. Stebe and

D. Lee, *Nature Communications*, 2017, **8**, 1234.

76 M. E. Cates and P. S. Clegg, *Soft Matter*, 2008, **4**, 2132.